НАУЧНО-ТЕХНИЧЕСКИЙ ВЕСТНИК ИНФОРМАЦИОННЫХ ТЕХНОЛОГИЙ, МЕХАНИКИ И ОПТИКИ
январь–февраль 2025 Том 25 № 1 http://ntv.ifmo.ru/
SCIENTIFIC AND TECHNICAL JOURNAL OF INFORMATION TECHNOLOGIES, MECHANICS AND OPTICS
January–February 2025 Vol. 25 No 1 http://ntv.ifmo.ru/en/
ISSN 2226-1494 (print) ISSN 2500-0373 (online)

НАУЧНО-ТЕХНИЧЕСКИЙ ВЕСТНИК
ИНФОРМАЦИОННЫХ ТЕХНОЛОГИЙ, МЕХАНИКИ И ОПТИКИ

doi: 10.17586/2226-1494-2025-25-1-78-86

Directional variance-based algorithm for digital image smoothing

Zohair Al-Ameen✉

ICT Research Unit, University of Mosul, Mosul, 41002, Iraq

qizohair@uomosul.edu.iq✉, https://orcid.org/0000-0003-3630-2134

Abstract

Image smoothing is vital in image processing as it attenuates the texture and unnecessary high-frequency components and provides a smooth image with a preserved structure to facilitate subsequent operations or analysis. Smoothed images are required in many image processing applications, such as details boost, sharpening, High Dynamic Range imaging, edge detection, stylization, abstraction, etc. Still, not all existing smoothing methods are successful in this task, as some undesirable problems may be introduced, such as removing significant details, introducing excessive blurring, processing flaws, halos, and other artifacts. Thus, the opportunity still stands to provide a new algorithm that smooths an image efficiently. This study concisely explores smoothing via the Directional Variances (DV) concept. The proposed algorithm leverages the DV concept to minimize energy, seeking a balance between essential structural preservation and smoothness. The proposed algorithm iteratively smooths the image using DV, diffusion, regularization, and energy minimization. A thorough evaluation is conducted on diverse images, showcasing the effectiveness of the developed algorithm. The results demonstrate that the developed DV-based algorithm has superb abilities in smoothing different images while preserving structural details, making it a valuable tool for various applications in digital image processing.

Keywords

Chan-Vese, regularization, image smoothing, diffusion, directional variance

Acknowledgments

I have heartfelt gratitude to the Computer Center staff for the aid that led to the completion of this research.

For citation: Zohair Al-Ameen. Directional variance-based algorithm for digital image smoothing. *Scientific and Technical Journal of Information Technologies, Mechanics and Optics*, 2025, vol. 25, no. 1, pp. 78–86. doi: 10.17586/2226-1494-2025-25-1-78-86

УДК 004.932

Алгоритм сглаживания цифровых изображений на основе дисперсии направлений

Зохаир Аль-Амин✉

Отделение информационных технологий Университета Мосула, Мосул, 41002, Ирак

qizohair@uomosul.edu.iq✉, https://orcid.org/0000-0003-3630-2134

Аннотация

Технология сглаживания изображений применяется при обработке изображений. Использование данной технологии ослабляет текстуру и ненужные высокочастотные компоненты, обеспечивает получение гладкого изображения с сохраненной структурой для облегчения последующих операций корректировки или анализа. Получение сглаженных изображений требуется во многих приложениях при обработке, например, High Dynamic Range изображений, при усилении деталей, повышении резкости, обнаружении краев, стилизации, абстракции и т. д. При этом, не все существующие методы сглаживания изображений успешно справляются с поставленной задачей. В результате могут возникнуть нежелательные проблемы, такие как удаление существенных деталей, введение чрезмерного размытия, дефекты обработки, ореолы и другие артефакты. В работе представлен новый алгоритм, который эффективно сглаживает изображение. Алгоритм основан на концепции направленных дисперсий (Directional Variances, DV) для минимизации энергии и получения баланса

между сохранением структуры и гладкостью. С помощью концепции DV представленный алгоритм итеративно сглаживает изображение, диффузии, осуществляет регуляризацию и минимизацию энергии. Выполненная оценка полученных результатов на различных изображениях показала эффективность разработанного алгоритма. Алгоритм на основе DV обладает превосходными возможностями сглаживания изображений, сохраняя при этом структурные детали, что делает его ценным инструментом для приложений, применяемых в области цифровой обработки изображений.

Ключевые слова
метод Чан-Везе, регуляризация, сглаживание изображений, диффузия, направленная дисперсия

Благодарности
Автор благодарен сотрудникам компьютерного центра Президентства Университета Мосула за помощь в завершении исследования.

Ссылка для цитирования: Зохаир Аль-Амин. Алгоритм сглаживания цифровых изображений на основе дисперсии направлений // Научно-технический вестник информационных технологий, механики и оптики. 2025. Т. 25, № 1. С. 78–86 (на англ. яз.). doi: 10.17586/2226-1494-2025-25-1-78-86

Introduction

Various real-life imaging applications demand the attenuation of insignificant information while maintaining significant structural details of an image, called image smoothing [1]. Smoothed images are required in many image processing applications, such as details boost, sharpening, pattern recognition, High Dynamic Range (HDR) imaging, edge detection, stylization, abstraction, matrix completion, image restoration, and more [2]. Image smoothing has been an active research topic for many years due to its importance in image processing, computer graphics, and computer vision. Its main goal is attenuating high-frequency components and textural information and maintaining the significant edges and structural information [3]. Because of its importance, dissimilar approaches have been developed in recent years. In 2016, a random walks-based algorithm was presented [4] which initiates by getting the selected image and the related parameters. Next, the weights for the image edges are determined using a Gaussian weighting approach. After that, the weighted adjacency array of the input image is constructed along with the diagonal array containing the degree of every used node. A particular minimization function is applied to smooth and generate the output image using this predetermined datum.

In 2017, a truncated total variation algorithm was introduced [5], starting by receiving the input image and the needed parameters. Next, the iteration begins, and the image is updated using the Euler-Lagrange approach followed by applying a unique minimizer to shrink the unwanted energies. After that, the image is modified using fixed solvers and total variation. This process is repeated until the iterations are finished and the output image is produced. In 2018, a sparse high-frequency gradient-based algorithm was created [6], wherein it initially decomposes the input image into high-frequency and constant components, in that the high-frequency is the non-smooth information and the constant is the smooth information. Next, the non-smooth information is eliminated if it has gradients with high frequency, and the other information is smoothed and combined with the sparse constraint to generate the resulting image.

In 2019, a 4th-order partial differential-based algorithm was proposed [7], starting by getting the input image and the required parameters related to the Gaussian kernel, fidelity, contrast, number of iterations, and the time step. A preprocessing phase begins by computing the diffusion tensor for every pixel, calculating the intensity change for each pixel, and updating the image accordingly. Next, the preprocessed image is fed to another iterative process which begins by computing the boundary conditions for each pixel, calculating two unique functions, and updating the image accordingly. The final image from the aforesaid iterative process is the resulting image. In 2020, a two-stage smoothing algorithm that depends on patch decomposition and histogram equalization was delivered [8], aiming to decrease the gradients of the textural details while increasing the gradient of significant structural edge details. The algorithm starts by dividing the input image into different patches, where the edge and textural information are concerted using a specialized segmentation process. The histogram equalization procedure is then applied to edge patches to improve the gradient of edges. Next, an L_0 gradient minimization approach is implemented to smooth each patch, and then an inverse equalization process is applied to ensure the edge boundary continuity. Finally, the overall image is filtered by an L_0 gradient minimization approach to attenuate the remaining textures and create the outcome.

In 2021, a multi-scale selective texture attenuation bested algorithm was developed [9], as it initially generates three scales of the image and applies Breadth-First Search (BFS) to purify the edges of the mid-scale. In addition, a mask that signifies non-texture and texture areas is extracted using BFS and an intuitive texture locator. This mask is then utilized to preserve structural information on the low scale and performs complete texture smoothing on the high scale. The output image is created by blending the outcomes of the masking operations. In 2022, a decomposition with a total variation-based algorithm was introduced [10], as it begins by increasing the difference between textural and structural details by applying a specialized filtering procedure. Next, the image is decomposed in the frequency domain with a limited multidirectional gradient, and the smooth elements are extracted. After that, the relative total variation approach is implemented on the smooth elements depending on the structural differences to attenuate the textural information while keeping the structural details. By iteratively performing these operations at different scales, the image is smoothed, and the resulting image is returned when the iterations end. In 2023, a weighted

sparse gradient-based algorithm was proposed [11], starting by suppressing gradients with low amplitude via an edge-aware mapping process. Next, the filtered gradients are sent to a weighted L_1 gradient remodeling phase to impose sparsity on the resulting gradients and enable the edge-aware feature. The resulting image is generated using a blend of Fourier optimization and augmented Lagrange multipliers.

The methods reviewed show that different processing concepts were used, but most are of high complexity and involve numerous computations. Still, the chance remains to introduce an algorithm that can smooth an image while preserving its main structure without using colossal computations. Thus, a Directional Variances (DV) based algorithm is developed to perform proper image smoothing while keeping structural details. The proposed algorithm iteratively smooths the image using DV, diffusion, regularization, and energy minimization. It has been tested by applying it on various images, checking the smoothing correctness visually and via the help of gradient maps and image evaluation methods through different iterations. The results obtained are promising, and an innovative processing concept for image smoothing has proved valid.

Proposed Algorithm

Digital images consist of two parts: color variations and structural details. The structural details are represented as edges in between the smooth variations. The color variations are termed Low-Frequency (LF) components, whereas the structural details are termed High-Frequency (HF) components. The LF components establish the base of the image, while the HF components are added to the image, providing the image details [12]. Hence, the HF components are more significant as they provide visible details to the image. The proposed algorithm is developed based on this notion by utilizing the DV concept to detect the overall HF information of the image so that such information is reduced to get the smoothed image that maintains the original structure of the input image.

The DV is a concept that has a tremendous ability to detect HF components in that it has different forms and methodologies to do so. The idea of the DV concept is to calculate differences between neighboring pixels in various directions to get the variance information which is deemed the HF components, then attenuate such components and create a simplified image representation. The Chan-Vese (CV) detectors (χ_1, χ_2, χ_3, and χ_4), which were initially designed for image segmentation, can provide reasonable performance in detecting the HF information by capturing the intensity differences and gradients. These detectors measure the differences in intensity and gradient magnitude in different directions, and they are expressed in [13] as:

$$\chi_1 = \frac{1}{\sqrt{\varepsilon^2 + (u^k_{i+1,j} - u^k_{i,j})^2 + \omega(u^k_{i,j+1} - u^k_{i,j-1})^2}}, \quad (1)$$

$$\chi_2 = \frac{1}{\sqrt{\varepsilon^2 + (u^k_{i,j} - u^k_{i-1,j})^2 + \omega(u^k_{i-1,j+1} - u^k_{i-1,j-1})^2}}, \quad (2)$$

$$\chi_3 = \frac{1}{\sqrt{\varepsilon^2 + \omega(u^k_{i+1,j} - u^k_{i-1,j})^2 + (u^k_{i,j+1} - u^k_{i,j})^2}}, \quad (3)$$

$$\chi_4 = \frac{1}{\sqrt{\varepsilon^2 + \omega(u^k_{i+1,j-1} - u^k_{i-1,j-1})^2 + (u^k_{i,j} - u^k_{i,j-1})^2}}, \quad (4)$$

where $u^k_{i,j}$ is the processed image at every iteration k; ω is a unique weight that is used to tune the detectors, in that it is set by default to $\omega = 0.25$; $\varepsilon = 10^{-5}$ small constant used to avoid division by zero; i, j are image coordinates; $f_{i,j}$ is the inputted image, in that $u^k_{i,j} = f_{i,j}$ is set at the first iteration; $u^k_{i,j}$ is the image in the original position; $u^k_{i+1,j}$ shifted up; $u^k_{i-1,j}$ shifted down; $u^k_{i,j+1}$ shifted right; $u^k_{i,j-1}$ shifted left; $u^k_{i-1,j+1}$ shifted down right; $u^k_{i-1,j-1}$ shifted down left, and $u^k_{i+1,j-1}$ shifted up left. These four CV detectors utilize the DV concept, wherein each CV detector is sensitive to intensity differences in a particular direction. Accordingly, χ_3 in Eq. (3) and χ_4 in Eq. (4) capture differences in the horizontal direction, while χ_1 in Eq. (1) and χ_2 in Eq. (2) capture differences in the vertical direction. Next, the output of the four CV detectors is refined by providing HF information reduction while preserving the edges using a Non-Linear Diffusion (NLD) procedure. The NLD helps maintain structural information, which is paramount, wherein regions with vital details undergo less smoothing, while areas with fewer details are more strongly smoothed. Those described above can be accomplished through exponential weighting that modulates the diffusion procedure. The standard NLD function can be expressed as in [14]:

$$D(|\nabla I|) = \exp\left(-\frac{\nabla I}{\alpha}\right), \quad (5)$$

where in Eq. (5) ∇ represents the gradient operator, α represents a diffusion parameter, and I represents the filtered image. This function is applied to the four CV detectors to refine their output, as discussed earlier, as defined below:

$$\bar{\chi}_1 = \chi_1 \exp\left(-\frac{|u^k_{i,j} - u^k_{i+1,j}|}{\alpha}\right), \quad (6)$$

$$\bar{\chi}_2 = \chi_2 \exp\left(-\frac{|u^k_{i,j} - u^k_{i-1,j}|}{\alpha}\right), \quad (7)$$

$$\bar{\chi}_3 = \chi_3 \exp\left(-\frac{|u^k_{i,j} - u^k_{i,j+1}|}{\alpha}\right), \quad (8)$$

$$\bar{\chi}_4 = \chi_4 \exp\left(-\frac{|u^k_{i,j} - u^k_{i,j-1}|}{\alpha}\right), \quad (9)$$

where in Eq. (6) to Eq. (9), α controls the strength of the diffusion (i.e., smoothness level), given that a higher value leads to more pronounced smoothness, a smaller value makes the diffusion procedure more sensitive to intensity variations. This scenario helps preserve fine details and edges since diffusion less influences adjacent pixels. Thus, using a lower α is preferable since, in this work, its value is set to ($\alpha = 0.5$). Next, the overall variance (χ_Λ) is computed, which represents all the HF information of the image is determined as each of the four detectors has a definite role in acquiring the variations. By computing χ_Λ, the influence of all four detectors is combined, allowing for

a balanced process between regularization and smoothing. The variance χ_Λ is calculated as follows [13]:

$$\chi_\Lambda = \bar{\chi}_1 + \bar{\chi}_2 + \bar{\chi}_3 + \bar{\chi}_4. \quad (10)$$

After that, the projection ($p_{i,j}^k$) is computed to guide the diffusion of pixel intensities during each iteration. Accordingly, in regions with significant intensity differences between the central pixel and its adjacent pixels, the component $p_{i,j}^k$ has significance, aiding in adjusting the value of the central pixel with the aid of the non-linearly diffused detectors. Those mentioned above can be done by using the following equation [15]:

$$p_{i,j}^k = (\bar{\chi}_1 u_{i+1,j}^k) + (\bar{\chi}_2 u_{i-1,j}^k) + (\bar{\chi}_3 u_{i,j+1}^k) + (\bar{\chi}_4 u_{i,j-1}^k). \quad (11)$$

Computing $p_{i,j}^k$ ensures that the smoothed areas retain similarity to the original structure which is an essential aspect of image smoothing. This is achieved by incorporating information from nearby pixels, including gradient and intensity information, allowing the local image structure to be considered when determining how pixel intensities should be modified. Next, a proper shrinking method must reduce the HF information while preserving essential details. The discrete forward update step of the CV segmentation method mentioned in [13] utilizes several aspects to refine the segmentation process. The update step is mathematically expressed as follows:

$$u_{i,j}^{k+1} = \quad (12)$$

$$= \frac{u_{i,j}^k + g(u^k) + \lambda\delta(u^k)[\chi_1 u_{i+1,j}^k + \chi_2 u_{i-1,j}^k + \chi_3 u_{i,j+1}^k + \chi_4 u_{i,j-1}^k]}{1 + \Delta t\delta(u^k)\lambda(\chi_1 + \chi_2 + \chi_3 + \chi_4)},$$

where ($u_{i,j}^{k+1}$) is the output of each iteration; $g(u^k)$ and $\delta(u^k)$ are parameters related to CV segmentation; Δt is responsible for the stability of segmentation, and parameter λ is accountable for the curve smoothness. Eq. (12) is used in image segmentation and needs to be modified to be more suitable for image smoothing. The part $[\chi_1 u_{i+1,j}^k + \chi_2 u_{i-1,j}^k + \chi_3 u_{i,j+1}^k + \chi_4 u_{i,j-1}^k]$ of Eq. (12) is like the projection mentioned in Eq. (11), and this part $(\chi_1 + \chi_2 + \chi_3 + \chi_4)$ of Eq. (12) is like Eq. (10) above. Thus, the components related to the segmentation are deleted, and Eq. (12) is remodeled to refine the image effectively and shrink the HF energy. With the refinement, a Laplacian regularization is applied to promote smoothness while reducing the built-up blur and preserving structural details. Moreover, it aims to prevent edges from being distorted when shrinking HF information. Edges are abrupt changes in intensity, and the Laplacian term is sensitive to these changes, helping to maintain them. The Laplacian regularization is the discrete Laplacian differential operator [16] that can be described using the following equation:

$$L_{i,j}^k = \left(\frac{(u_{i+1,j}^k + u_{i-1,j}^k + u_{i,j+1}^k + u_{i,j-1}^k)}{4}\right) - u_{i,j}^k. \quad (13)$$

The shrinking function is mainly utilized to determine how to update the pixel intensities for every iteration to achieve the desired level of smoothness. The remodeled shrinking function can now be described using the following formula:

$$u_{i,j}^{k+1} = \frac{u_{i,j}^k + (\lambda p_{i,j}^k) - (\lambda L_{i,j}^k)}{1 + (\lambda\chi_\Lambda)}, \quad (14)$$

where λ is a smoothness factor that satisfies ($\lambda = 0.1$), Eq. (14) balances the influence of non-linear diffused detectors $\bar{\chi}_1$, $\bar{\chi}_2$, $\bar{\chi}_3$, $\bar{\chi}_4$ with the Laplacian regularization term by ensuring both data fidelity (as captured by the non-linear diffused detectors) and structural coherence (as facilitated by Laplacian regularization) are considered during the smoothing (update) process. Likewise, Eq. (14) enables adaptive smoothing by adapting to the local context. Accordingly, it allows for more controlled updates to preserve features for regions with high-intensity variations such as edges. In contrast, it will enable substantial updates for regions with low-intensity variations, helping to reduce unwanted variations and enabling better smoothness.

Moreover, updating intensities based on a balance between the data-driven term (diffused detectors) and regularization term (Laplacian regularization) allows for preserving the coherence and consistency of the image shape. The algorithm iteratively updates the image by considering the local image properties. The loop stays for a given number of iterations, and after all iterations end, the smoothed image ($u_{i,j}^{k+1}$) is returned. The final step involves the application of the standard median filter [17] to eliminate some speckle-like artifacts and deliver the final output image.

To methodically explain how the developed algorithm works, it starts by getting image $f_{i,j}$ as input, and the number of iterations, which signifies a user-defined parameter controlling the smoothing amount, where a higher value results in more robust smoothing. Next, it sets the values of α, ω, λ, ε, and ($u_{i,j}^k = f_{i,j}$). The algorithm core lies in the iterative loop that starts by computing the four CV detectors via Eqs (1)–(4). Next, the non-linear diffused CV detectors are calculated via Eqs (6)–(9), along with the overall variance using Eq. (10). Afterwards, the projection is determined using Eq. (11), the Laplacian regularization term is calculated via Eq. (13) followed by the implementation of the shrinking function via Eq. (14). These computations are repeated, the loop continues until all iterations are completed, wherein the standard median filter is applied once on the resulted image ($u_{i,j}^{k+1}$) as a last step to generate the output image. Lastly, the structural outline of the developed algorithm is given in Fig. 1.

Results and Discussion

This section is dedicated to the dataset, evaluation methods, experimental results, and the needed analysis. The dataset used in this study is Microsoft Common Objects in Context (COCO) [18]. The COCO dataset is intended for object detection, containing more than 330k images of various scenes with different sizes, wherein more than three hundred images from this dataset were used in this study. Visual and objective assessment methods were used in addition to CPU runtimes for quality evaluation. All developments and experiments were conducted using a

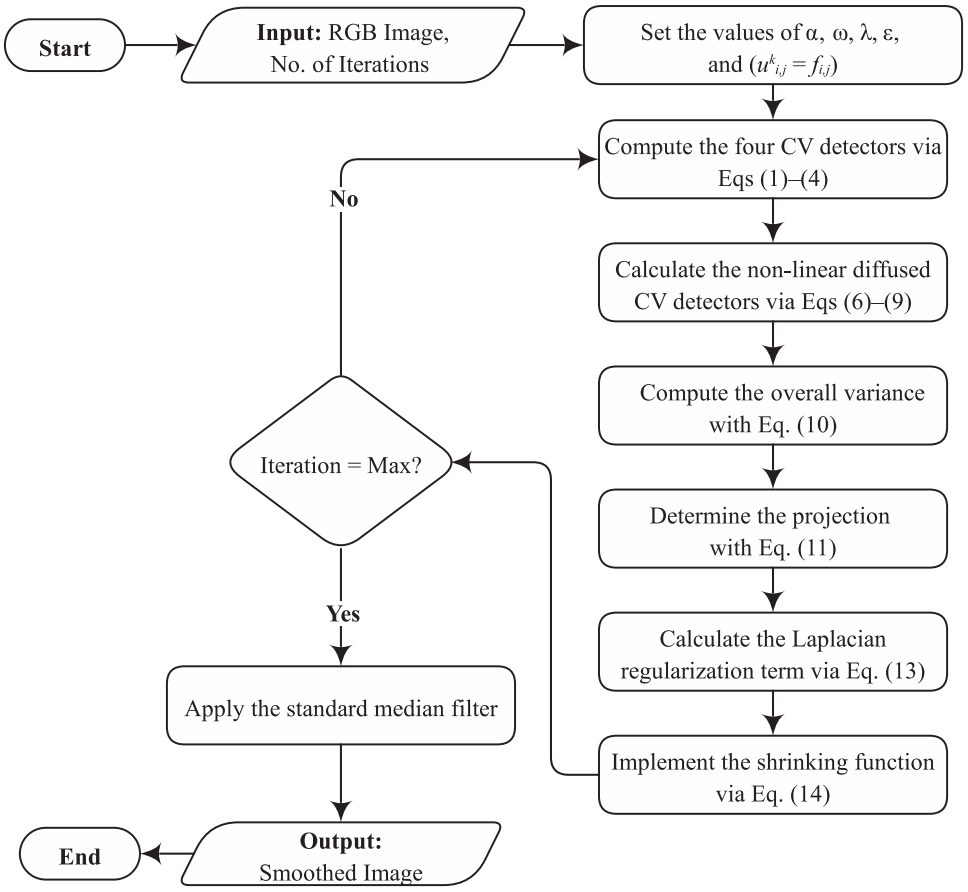

Fig. 1. Structural outline of the introduced DV-based algorithm

laptop with an AMD Ryzen 7 Pro 4750U 1.70 GHz CPU and 32.0 GB of RAM. As for visual assessment, the gradient maps of the output images with a jet color scheme are utilized to better represent structural information and the variations by assigning colors to different values [8]. This can be helpful in visually highlighting the various levels of structural information and variations in an image. The jet color scheme has been utilized in scientific visualization for a long time and has become standard. For objective evaluation, the Average Local Binary Pattern (ALBP) [19] and Mean Gradient Magnitude (MGM) [20] measures have been used to evaluate the textural and HF information of the algorithm across different iterations. ALBP is used to measure textural details as it could provide insights into the impact of smoothing on texture, in that the more texture the algorithm attenuates, the more smoothness occurs.

MGM evaluates the HF information, indicating the gradient strength over the entire image. When an image is smoothed, the gradient magnitude is indirectly affected, resulting in a reduction in gradient magnitude. ALBP and MGM are no-reference assessment methods, wherein a lower value indicates less texture and HF information

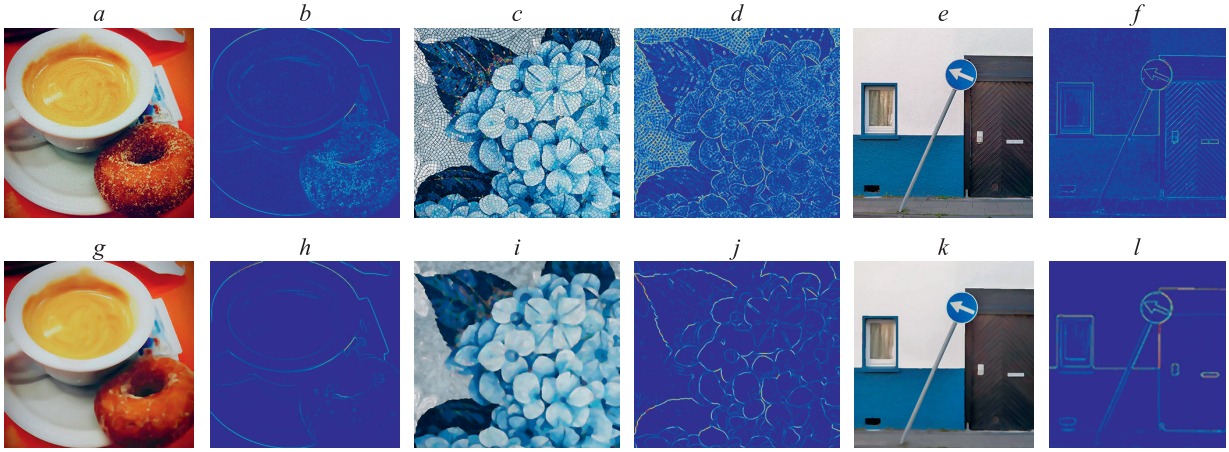

Fig. 2. Experimental results with gradient maps. Original images (*a*, *c*, *e*); gradient maps of the original images (*b*, *d*, *f*); smoothed images using different iteration values (70, 50, 60) (*g*, *i*, *k*); gradient maps of the smoothed images (*h*, *j*, *l*)

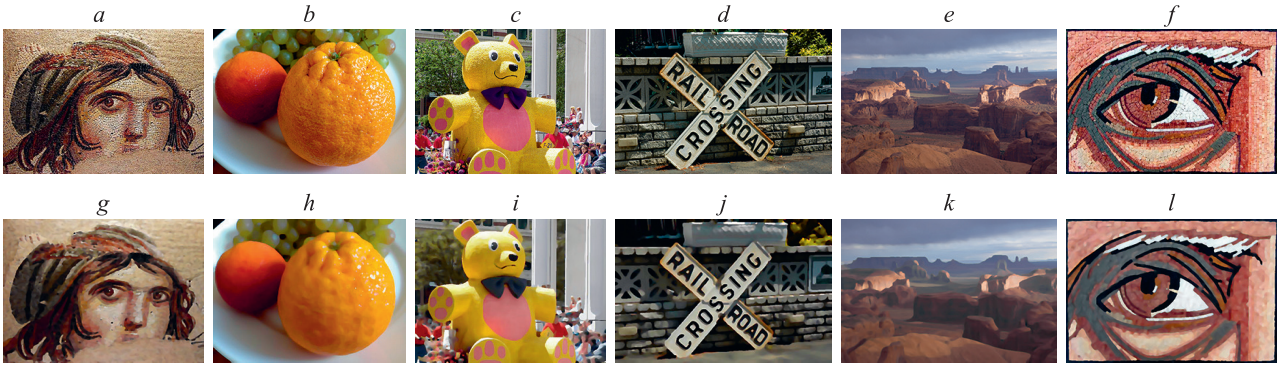

Fig. 3. Experimental results of smoothing different images (**Batch 1**). Original images (*a–f*); the smoothing results using different iteration values (50, 80, 60, 70, 50, 80), respectively (*g–l*)

appearance in the smoothed images. As for CPU runtime, it is used to show the computational complexity of the proposed algorithm [21]. The results of the experiments can be seen in Fig. 2 to Fig. 6 and the given Table. As seen in Fig. 2, different images with dissimilar textures have been smoothed by the DV algorithm, where the HF components of the images were significantly reduced, and the output images contain the vital structural components as demonstrated by the before and after gradients maps of each considered image. The gradient maps highlighted the structural information of the smoothed images clearly, helping to identify and describe their essential patterns, wherein their discriminative features clearly show the success of the algorithm in reducing the HF information while retaining the critical image details as the bright areas represent regions with high variations, while darker areas correspond to smoothed regions.

Fig. 3 and Fig. 4 show the results of smoothing different images using the developed algorithm. As observed, the proposed algorithm is successful in smoothing images with various textures and details, attenuating the HF information and retaining their fundamental structures. To further investigate the performance of the developed DV-based algorithm, an experiment that includes smoothing an image with different iterations and providing the corresponding gradient map for each output is delivered to comprehend various behavioral issues regarding the required time, the amount of texture and HF information attenuation when increasing the iterations. Fig. 5 demonstrates the experiment outcome with the related gradient maps. The Table provides the assessment readings and runtimes through different iterations. Fig. 6 shows a graphical representation of iterations vs quality evaluation readings.

From the experiments conducted, it can be observed that the runtimes increase almost linearly when the iteration number increases. Moreover, the readings of the ALBP indicate that the developed algorithm can attenuate the texture even after more iterations are utilized, and the decrease in textural information is somewhat straight. As for MGM, the readings indicate that the ability of the developed algorithm to reduce HF information is strongly present. The significant processing happens in the first 150

Fig. 4. Experimental results of smoothing different images (**Batch 2**). Original images (*a–f*); the smoothing results using different iteration values (35, 60, 30, 30, 40, 50), respectively (*g–l*)

Fig. 5. Showing the proposed algorithm smoothing abilities with the gradient maps via different numbers of iterations. Original image (*a*); images (*b–f*) and (*m–r*) are smoothed images starting at 25 iterations and ending at 275 iterations with an increase of 25; the gradient maps (*g–l*) of images (*a–f*); the gradient maps (*s–x*) of images (*m–r*)

Table. Quality evaluation and runtimes via iterations

Iterations	ALBP	MGM	Runtimes, s
25	0.0976	0.058585	2.159024
50	0.0950	0.047315	4.066738
75	0.0910	0.041448	5.986797
100	0.0869	0.037540	7.933668
125	0.0825	0.034665	9.804604
150	0.0780	0.032452	11.739654
175	0.0738	0.030690	13.633869
200	0.0699	0.029532	15.600377
225	0.0664	0.028549	17.460385
250	0.0634	0.027893	19.526623
275	0.0609	0.027189	21.328536

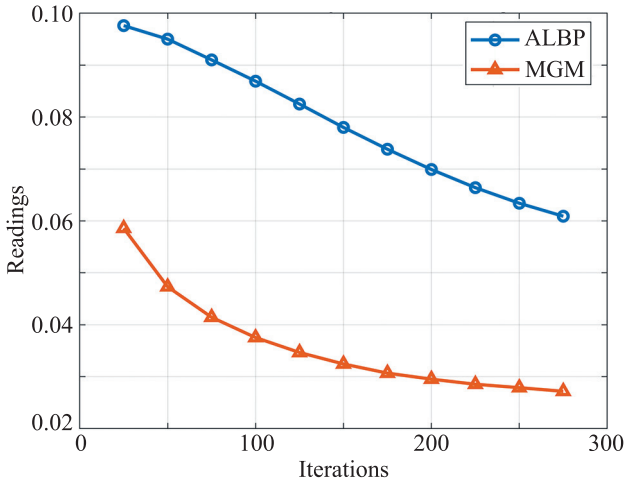

Fig. 6. Readings of the quality evaluation methods through different iterations

iterations and begins to decrease after that due to structural preservation supported by the algorithm.

As seen in the gradient maps in Fig. 5, *g–l*, and Fig. 5, *s–x*, the effect of attenuating textural and HF information can be seen. The processing ability of the developed algorithm is evident in that the structural, textural, and HF information are mixed in the gradient map in Fig. 5, *g*. Throughout the iterations, the primary structural details began to be distinguished as textural, and HF information was attenuated. The last gradient map in Fig. 5, *x* shows only the primary structural details of the image, indicating that the proposed algorithm is successful in its smoothing task.

Conclusion

This paper presents a Directional Variances (DV) based algorithm for image smoothing that iteratively refines the image via the DV concept, diffusion, regularization, and energy minimization. The DV is used to capture the High-Frequency (HF) information, the diffusion is applied to facilitate the smoothing process, the regularization reduces the built-up blur, and the energy minimization utilizes those as mentioned earlier to reduce the HF and textural information. The iterative feature allows for continuous refinement until the anticipated level of smoothness is attained. The developed algorithm has been tested with

different images checked using various numbers of iterations with gradient maps and two assessment methods. The results showed promising abilities as the DV algorithm enabled adequate textural and HF information attenuation through a computationally efficient algorithm, in that the output images showed efficiency in reducing the irregularities in images. This is uneasy as many existing image-smoothing algorithms have high computational costs. Finally, the future directions regarding this study can be the autonomous determination of required iterations so that it becomes a self-regulating algorithm.

References

1. Sun X., Lv X., Zhu G., Fang B., Jiang L. Fast additive half-quadratic iterative minimization for lp — lq image smoothing. *IET Image Processing*, 2023, vol. 17, no. 6, pp. 1739–1751. https://doi.org/10.1049/ipr2.12751
2. Huang J., Wang H., Wang X., Ruzhansky M. Semi-sparsity for smoothing filters. *IEEE Transactions on Image Processing*, 2023, vol. 32, pp. 1627–1639. https://doi.org/10.1109/TIP.2023.3247181
3. Liu W., Zhang P., Huang X., Yang J., Shen C., Reid I. Real-time image smoothing via iterative least squares. *ACM Transactions on Graphics*. 2020, vol. 39, no. 3, pp. 1–24. https://doi.org/10.1145/3388887
4. Wang Z., Wang H. Image smoothing with generalized random walks: Algorithm and applications. *Applied Soft Computing*, 2016, vol. 46, pp. 792–804. https://doi.org/10.1016/j.asoc.2016.01.003
5. Dou Z., Song M., Gao K., Jiang Z. Image Smoothing via Truncated Total Variation. *IEEE Access*, 2017, vol. 5, pp. 27337–27344. https://doi.org/10.1109/access.2017.2773503
6. Ma G.H., Zhang M.L., Li X.M., Zhang C.M. Image smoothing based on image decomposition and sparse high frequency gradient. *Journal of Computer Science and Technology*, 2018, vol. 33, no. 3, pp. 502–510. https://doi.org/10.1007/s11390-018-1834-3
7. Wang N., Chen Y., Yao L., Zhang Q., Jia L., Gui Z. Image smoothing via adaptive fourth-order partial differential equation model. *Journal of Engineering*, 2019, vol. 2019, no. 11, pp. 8198–8206. https://doi.org/10.1049/joe.2018.5443
8. Liu Y., Ma X., Li X., Zhang C. Two-stage image smoothing based on edge-patch histogram equalisation and patch decomposition. *IET Image Processing*. 2020, vol. 14, no. 6, pp. 1132–1140. https://doi.org/10.1049/iet-ipr.2019.0484
9. Liu C., Feng Y., Yang C., Wei M., Wang J. Multi-scale selective image texture smoothing via intuitive single clicks. *Signal Processing: Image Communication*, 2021, vol. 97, pp. 116357. https://doi.org/10.1016/j.image.2021.116357
10. Ye-Peng L., De-Zhi Y., Si-Yuan L., Fan Z., Cai-Ming Z. Image smoothing based on image decomposition and relative total variation. *Journal of Graphics*, 2022, vol. 43, no. 6, pp. 1143–1149. https://doi.org/10.11996/JG.j.2095-302X.2022061143
11. Zeng L., Chen Y., Yang Y., Pan Z. Edge-aware image smoothing via weighted sparse gradient reconstruction. *Signal, Image and Video Processing*, 2023, vol. 17, no. 8, pp. 4285–4293. https://doi.org/10.1007/s11760-023-02661-5
12. Zuo Z., Lan X., Deng L., Yao S., Wang X. An improved medical image compression technique with lossless region of interest. *Optik*, 2015, vol. 126, no. 21, pp. 2825–2831. https://doi.org/10.1016/j.ijleo.2015.07.005
13. Beylerian E. Finding a needle in a haystack: An image processing approach. *SIAM Undergraduate Research Online*, 2013, vol. 6, pp. 54–66. https://doi.org/10.1137/12s0119008
14. Ghita O., Robinson K., Lynch M., Whelan P.F. MRI diffusion-based filtering: a note on performance characterization. *Computerized Medical Imaging and Graphics*, 2005, vol. 29, no. 4, pp. 267–277. https://doi.org/10.1016/j.compmedimag.2004.12.003
15. Wang J., Lucier B.J. Error bounds for finite-difference methods for Rudin–Osher–Fatemi image smoothing. *SIAM Journal on Numerical Analysis*, 2011, vol. 49, no. 2, pp. 845–868. https://doi.org/10.1137/090769594
16. Wan M., Zhao D., Zhao B. Combining Max pooling-Laplacian theory and k-means clustering for novel camouflage pattern design. *Frontiers in Neurorobotics*, 2022, vol. 16, pp. 1041101. https://doi.org/10.3389/fnbot.2022.1041101
17. Fahnun B.U., Andani L.S., Fadlillah H.M., Putra H.D. Color image enhancement using filtering and contrast enhancement. *Jurnal Mantik*, 2023, vol. 7, no. 1, pp. 177–184. https://doi.org/10.35335/mantik.v7i1.3678

Литература

1. Sun X., Lv X., Zhu G., Fang B., Jiang L. Fast additive half-quadratic iterative minimization for lp — lq image smoothing // IET Image Processing. 2023. V. 17. N 6. P. 1739–1751. https://doi.org/10.1049/ipr2.12751
2. Huang J., Wang H., Wang X., Ruzhansky M. Semi-sparsity for smoothing filters // IEEE Transactions on Image Processing. 2023. V. 32. P. 1627–1639. https://doi.org/10.1109/TIP.2023.3247181
3. Liu W., Zhang P., Huang X., Yang J., Shen C., Reid I. Real-time image smoothing via iterative least squares // ACM Transactions on Graphics. 2020. V. 39. N 3. P. 1–24. https://doi.org/10.1145/3388887
4. Wang Z., Wang H. Image smoothing with generalized random walks: Algorithm and applications // Applied Soft Computing. 2016. V. 46. P. 792–804. https://doi.org/10.1016/j.asoc.2016.01.003
5. Dou Z., Song M., Gao K., Jiang Z. Image Smoothing via Truncated Total Variation // IEEE Access. 2017. V. 5. P. 27337–27344. https://doi.org/10.1109/access.2017.2773503
6. Ma G.H., Zhang M.L., Li X.M., Zhang C.M. Image smoothing based on image decomposition and sparse high frequency gradient // Journal of Computer Science and Technology. 2018. V. 33. N 3. P. 502–510. https://doi.org/10.1007/s11390-018-1834-3
7. Wang N., Chen Y., Yao L., Zhang Q., Jia L., Gui Z. Image smoothing via adaptive fourth-order partial differential equation model // Journal of Engineering. 2019. V. 2019. N 11. P. 8198–8206. https://doi.org/10.1049/joe.2018.5443
8. Liu Y., Ma X., Li X., Zhang C. Two-stage image smoothing based on edge-patch histogram equalisation and patch decomposition // IET Image Processing. 2020. V. 14. N 6. P. 1132–1140. https://doi.org/10.1049/iet-ipr.2019.0484
9. Liu C., Feng Y., Yang C., Wei M., Wang J. Multi-scale selective image texture smoothing via intuitive single clicks // Signal Processing: Image Communication. 2021. V. 97. P. 116357. https://doi.org/10.1016/j.image.2021.116357
10. Ye-Peng L., De-Zhi Y., Si-Yuan L., Fan Z., Cai-Ming Z. Image smoothing based on image decomposition and relative total variation // Journal of Graphics. 2022. V. 43. N 6. P. 1143–1149. https://doi.org/10.11996/JG.j.2095-302X.2022061143
11. Zeng L., Chen Y., Yang Y., Pan Z. Edge-aware image smoothing via weighted sparse gradient reconstruction // Signal, Image and Video Processing. 2023. V. 17. N 8. P. 4285–4293. https://doi.org/10.1007/s11760-023-02661-5
12. Zuo Z., Lan X., Deng L., Yao S., Wang X. An improved medical image compression technique with lossless region of interest // Optik. 2015. V. 126. N 21. P. 2825–2831. https://doi.org/10.1016/j.ijleo.2015.07.005
13. Beylerian E. Finding a needle in a haystack: An image processing approach // SIAM Undergraduate Research Online. 2013. V. 6. P. 54–66. https://doi.org/10.1137/12s0119008
14. Ghita O., Robinson K., Lynch M., Whelan P.F. MRI diffusion-based filtering: a note on performance characterization // Computerized Medical Imaging and Graphics. 2005. V. 29. N 4. P. 267–277. https://doi.org/10.1016/j.compmedimag.2004.12.003
15. Wang J., Lucier B.J. Error bounds for finite-difference methods for Rudin–Osher–Fatemi image smoothing // SIAM Journal on Numerical Analysis. 2011. V. 49. N 2. P. 845–868. https://doi.org/10.1137/090769594
16. Wan M., Zhao D., Zhao B. Combining Max pooling-Laplacian theory and k-means clustering for novel camouflage pattern design // Frontiers in Neurorobotics. 2022. V. 16. P. 1041101. https://doi.org/10.3389/fnbot.2022.1041101
17. Fahnun B.U., Andani L.S., Fadlillah H.M., Putra H.D. Color image enhancement using filtering and contrast enhancement // Jurnal Mantik. 2023. V. 7. N 1. P. 177–184. https://doi.org/10.35335/mantik.v7i1.3678

18. Lin T.Y., Maire M., Belongie S., Hays J., Perona P., Ramanan D., Dollár P., Zitnick C.L. Microsoft COCO: Common objects in context. *Lecture Notes in Computer Science*, 2014, vol. 8693, pp. 740–755. https://doi.org/10.1007/978-3-319-10602-1_48
19. Singh K.R., Chaudhury S. Comparative analysis of texture feature extraction techniques for rice grain classification. *IET Image Processing*, 2020, vol. 14, no. 11, pp. 2532–2540. https://doi.org/10.1049/iet-ipr.2019.1055
20. Li C., Ju Y., Bovik A.C., Wu X., Sang Q. No-training, no-reference image quality index using perceptual features. *Optical Engineering*, 2013, vol. 52, no 5, pp. 057003. https://doi.org/10.1117/1.oe.52.5.057003
21. Yang Y., He T., Zeng L., Zhao Y., Wang X. Soft clustering based on high- and low-level features for image smoothing. *Journal of Electronic Imaging*, 2023, vol. 32, no. 1, pp. 013028. https://doi.org/10.1117/1.jei.32.1.013028

18. Lin T.Y., Maire M., Belongie S., Hays J., Perona P., Ramanan D., Dollár P., Zitnick C.L. Microsoft COCO: Common objects in context // Lecture Notes in Computer Science. 2014. V. 8693. P. 740–755. https://doi.org/10.1007/978-3-319-10602-1_48
19. Singh K.R., Chaudhury S. Comparative analysis of texture feature extraction techniques for rice grain classification // IET Image Processing. 2020. V. 14. N 11. P. 2532–2540. https://doi.org/10.1049/iet-ipr.2019.1055
20. Li C., Ju Y., Bovik A.C., Wu X., Sang Q. No-training, no-reference image quality index using perceptual features // Optical Engineering. 2013. V. 52. N 5. P. 057003. https://doi.org/10.1117/1.oe.52.5.057003
21. Yang Y., He T., Zeng L., Zhao Y., Wang X. Soft clustering based on high- and low-level features for image smoothing // Journal of Electronic Imaging. 2023. V. 32. N 1. P. 013028. https://doi.org/10.1117/1.jei.32.1.013028

Author

Zohair Al-Ameen — PhD (Computer Science), Associate Professor, Researcher, ICT Research Unit, University of Mosul, Mosul, 41002, Iraq, SC 55377732400, https://orcid.org/0000-0003-3630-2134, qizohair@uomosul.edu.iq

Автор

Зохаир Аль-Амин — PhD (компьютерные технологии), доцент, исследователь, Отделение информационных технологий Университета Мосула, Мосул, 41002, Ирак, SC 55377732400, https://orcid.org/0000-0003-3630-2134, qizohair@uomosul.edu.iq

Received 23.10.2024
Approved after reviewing 13.12.2024
Accepted 22.01.2025

Статья поступила в редакцию 23.10.2024
Одобрена после рецензирования 13.12.2024
Принята к печати 22.01.2025